Work Strengthening in a Fe-Ni-Co-Cr-Mo Alloy

H. T. MICHELS AND R. M. FORBES JONES

The effect of cold work on the mechanical properties and microstructure of an fcc Fe-Ni-Co-Cr-Mo alloy is discussed. In samples deformed up through 20 pct, strengthening is attributed to an increase in dislocation content. Greater deformation (48 and 75 pct) results in the formation of deformation twins which increase in density with cold working. The deformation twins contribute to the high yield strength (0.2 pct offset) of 154 kg/mm^2 which is attained in this alloy upon cold working (75 pct elongation). This hardening mechanism is in contrast with that reported to be operating in a similar fcc Co-Ni-Cr-Mo alloy in which strengthning is attributed to the formation of a deformation-induced fine hcp epsilon phase.

IN the course of examining an experimental high strength Fe-25 Ni-21 Co-20 Cr-8 Mo alloy, initial observations indicated that its microstructure was similar to that of MP 35N.* The latter Co-35 Ni-20 Cr-10 Mo alloy, one of a family designated MULTIPHASE,* is reported[3] to derive its strength mainly from the formation of a fine hcp epsilon phase during room temperature mechanical working. Closer investigation of the structure of the Fe-25 Ni-21 Co-20 Cr-8 Mo alloy indicated that indeed, epsilon does not form in this case. However, in contrast to MP 35N, strengthening of the Fe-25 Ni-21 Co-20 Cr-8 Mo alloy is attributed to the formation of mechanical twins which increase in density with higher deformation. These twins subdivide the matrix and are functionally equivalent to grain refinement in that they act as obstacles to dislocation motion. This investigation is concerned with the origin, nature and characteristics of the structure which develops in this alloy as a function of cold work.

*Trademark of Standard Pressed Steel Co., Jenkentown, Penn.

EXPERIMENTAL PROCEDURE

Table I gives the composition of the alloy which was air induction-melted as a 136-kg (300-lb) heat, deoxidized with aluminum and poured at 1549°C (2820°F). The 15.2 cm by 15.2 cm (6 in. by 6 in.) ingot was homogenized for 4 h at 1177°C (2150°F), hammer forged to 10.2 cm by 10.2 cm (4 in. by 4 in.), air cooled and cut in two.

The ingot was processed to bar by two routes. The first path was hot rolling to 15.9 mm (5/8 in.) square and machining to 12.7 mm (1/2 in.) round bar for cold drawing. Plates for sheet tensile specimens were prepared by the second route. This consisted of hot rolling plate to 19 mm (3/4 in.), cold rolling to 6.4 mm (1/4 in.), and surface grinding to the finished tensile specimen thickness of 3.6 mm (0.140 in.). All material was solution annealed for 1 h at 1204°C (2200°F) followed by a water quench prior to further mechanical working.

In preparation for electron metallography, annealed sheet tensile specimens were uniformly elongated by 3, 10, and 20 pct over a 2.54 cm (1 in.) gage length as monitored with an extensometer. Greater amounts of uniform deformation, equivalent to elongations of 48 and 75 pct were obtained by cold drawing from 12.7 mm (1/2 in.) round rod.

Samples for optical metallography were etched with a 10 pct chromic acid-water solution. Specimens for transmission electron microscopy were pre-dished in Disa A-2 solution and final thinning was carried out in 10 pct perchloric-acetic acid.

RESULTS

Microstructure

The annealed alloy is typical of a single phase austenitic material consisting of equiaxed grains with many annealing twins. Electron metallography revealed dissociated dislocations in the form of nodes as illustrated in Fig. 1. Calculation of stacking fault energy (γ) from these configurations[1] resulted in the values of approximately 18 ergs/cm^2. This is a low stacking fault energy and is in good agreement with the value of 15 ergs/cm^2 which is given by Friedel[2] for Fe-Ni-Cr (stainless steel), and is reasonably close to the 25 ergs/cm^2 value reported by Drapier, Viatour, Contsourdis, and Habraken[3] for MP 25N.

Light metallography revealed no microstructural change after tensile elongations of 3, 10, and 20 pct. However, electron metallography demonstrated that, as expected, the density of planar dislocation arrays increased with increased tensile deformation up to 20 pct elongation. An example of a typical dislocation structure after 10 pct tensile elongation is given in Fig. 2.

Deformation by cold drawing (48 and 75 pct) resulted in a markedly different microstructure. The light micrograph in Fig. 3 indicates that 48 pct deformation (by cold drawing) elongated the grains in the direction of working. In addition the individual grains contained many fine parallel striations. The striations have been associated with the formation of hcp epsilon

Table I. Chemical Composition of Fe-25Ni-20Co-20Cr-8Mo Alloy

(Wt Pct)												
Fe	Ni	Co	Cr	Mo	C	Mn	Si	Al	Ca	Mg	P	S
Bal	25.3	20.7	19.9	8.2	0.017	0.32	0.35	0.075	0.02	0.024	0.017	0.018

H. T. MICHELS and R. M. FORBES JONES are with The International Nickel Company, Inc., Paul D. Merica Research Laboratory, Sterling Forest, Suffern, N. Y. 10901.

Manuscript submitted August 6, 1973.

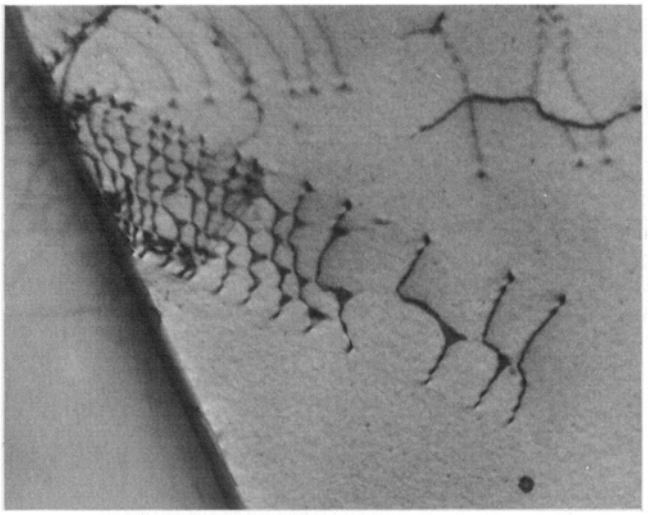

Fig. 1—Dislocation nodes observed in an annealed Fe-25 Ni-21 Co-20 Cr-8 Mo alloy. Magnification 45,000 times.

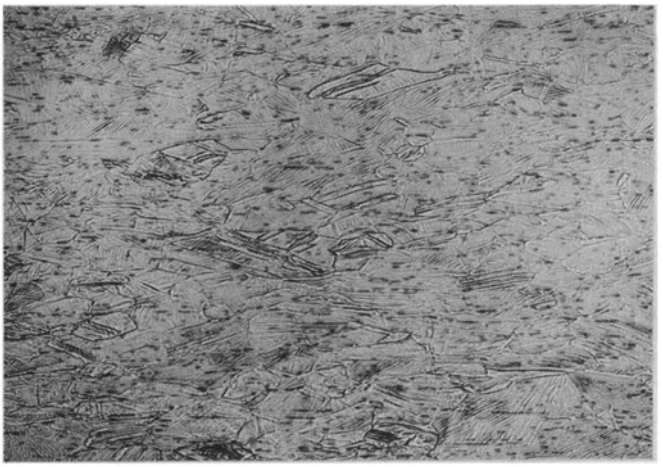

Fig. 3—Light micrograph of an Fe-25 Ni-21 Co-20 Cr-8 Mo alloy after 48 pct deformation (by cold drawing) showing grain elongation in the direction of cold work and many fine parallel striations within individual grains. Magnification 53 times.

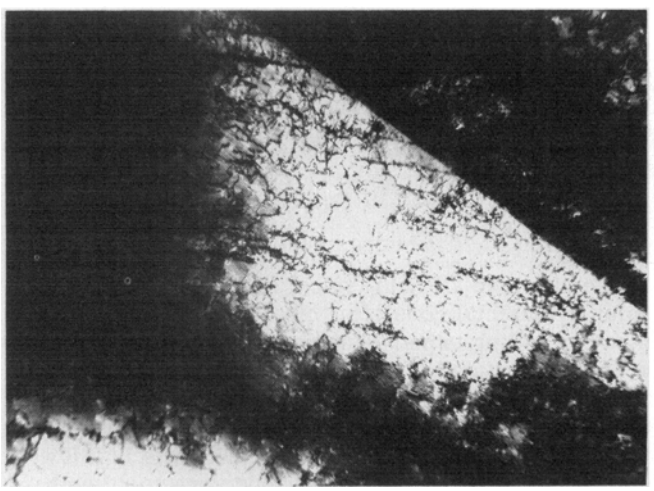

Fig. 2—Electron micrograph of an Fe-25 Ni-21 Co-20 Cr-8 Mo alloy illustrating a typical dislocation structure after 10 pct tensile deformation. Magnification 23,000 times.

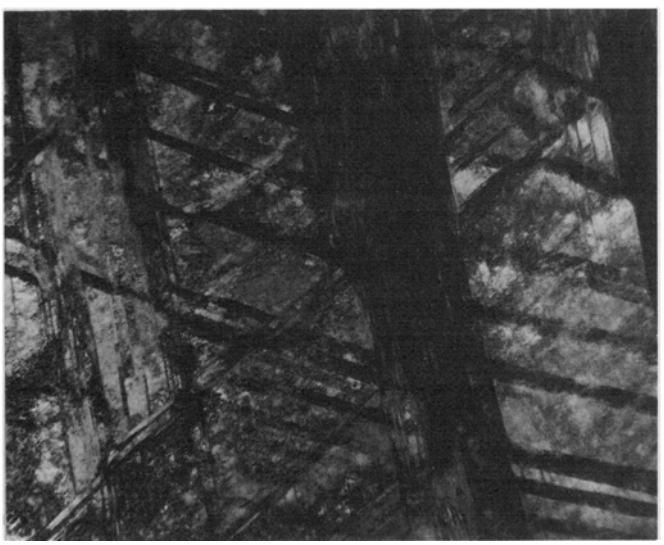

Fig. 4—Electron micrograph of an Fe-25 Ni-21 Co-20 Cr-8 Mo alloy after 48 pct deformation (by cold drawing) showing many fine platelets. Magnification 15,000 times.

by Drapier *et al*,[3] in MP35N but could also be related to mechanical twins. Although the structure which developed after 75 pct deformation (by cold drawing) could not be fully resolved by light metallography, both grain elongation and number of striations in grains appeared to increase. The inability of etchants to bring out the true structure is an indication of high and very uniform corrosion resistance and suggests that the deformed structure may be single phase. Transmission electron microscopy of the 48 pct cold drawn alloy (Fig. 4) revealed many fine platelets, which are presumably related to the striations observed in light metallography. In addition, the mottled appearance gave evidence that the area between the platelets had deformed. Increased cold drawing (75 pct) resulted in an increase in the number of platelets and a corresponding decrease in the interplate spacing (Fig. 5). The companion electron diffraction pattern which is inserted into Fig. 5 showed that the individual diffraction spots were elongated and tended to form continuous rings. This can be attributed to orientation variations from one platelet to another as a result of nonuniform strain.

Platelets were only observed in the cold drawn rod and not in the samples deformed up to 20 pct by tensile elongation. This is believed to be a consequence of the extent rather than the mode of the deformation, since platelets have also been observed in the necked region of annealed tensile specimens after they were pulled to failure (Fig. 6).

Work Strengthening

The hardness and microstructure developed in the alloy as a function of deformation are presented in Fig. 7. In those samples deformed up through 20 pct elongation, strengthening is attributed to increased dislocation content. At some point between 20 and 48 pct, dislocation motion becomes so difficult that the

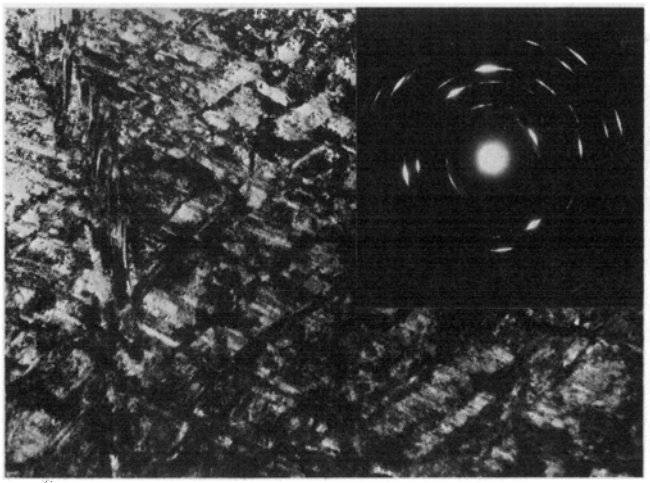

Fig. 5—Electron micrograph of an Fe-25 Ni-21 Co-20 Cr-8 Mo alloy after 75 pct deformation (by cold drawing) illustrating an increase in the platelet density. Magnification 21,500 times.

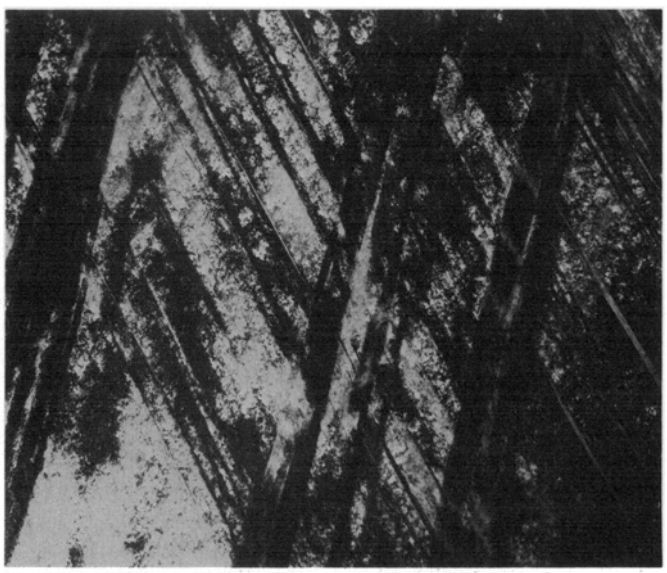

Fig. 6—Electron micrograph taken on area adjacent to necked region of annealed Fe-25 Ni-21 Co-20 Cr-8 Mo tensile specimen loaded to failure indicating that platelets form as a result of extent rather than mode of deformation. Magnification 7800 times.

formation of the platelets is the favored deformation process. Beyond 48 pct, strengthening is a result of an increase in platelet density.

Mechanical working at room temperature resulted in a five-fold increase in yield strength (0.5 pct offset) from 31 kg/mm^2 (44 ksi) in the annealed state to 154 kg/mm^2 (210 ksi) after 75 pct uniform deformation by cold drawing. Moreover an ultimate tensile strength of 180 kg/mm^2 (258 ksi) was achieved along with adequate ductility as indicated by an 11 pct elongation and a 38 pct reduction in area.

Nature of Platelets

A bright field image (Fig. 8(*a*)) of a sample after 48 pct deformation (by cold drawing) was taken on a region of the foil with a lower-than-average density of platelets. This region was chosen to simplify and

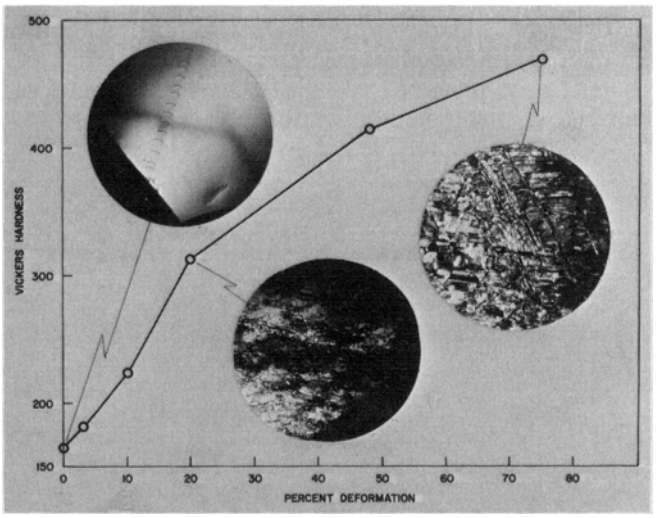

Fig. 7—Hardness response and microstructure developed as a function of deformation. Microstructure at approximately magnification 6500 times.

facilitate the analysis since only one family of platelets was present. The resulting electron diffraction pattern and interpretation are given in Figs. 8(*b*) and 8(*c*), respectively. It is a normal 110 type diffraction pattern found in fcc metals with superimposed twin spots with the following orientation relationship:

(111) twin plane parallel to (111) matrix plane, and
$[0\bar{1}1]$ twin direction parallel to $[0\bar{1}1]$ matrix direction.

Analysis performed on other regions with a higher but normal density of platelets yielded the same results. In Figs. 4 and 5 there are three platelet orientations. These correspond to twins on three of the four (111) type planes (the fourth being approximately parallel to the foil plane). The streaking in the [111] direction which is observed in the diffraction pattern (Fig. 8(*b*)) is a further indication that the broad face of the twin is on the (111) plane.

Dark field images were obtained from both matrix and twin reflections but only the latter is presented (Fig. 8(*d*)). Note that the twins are bright while the matrix is dark, thus illustrating that the twins are in a diffracting condition. Of course, a negative of Fig. 8(*d*), that is, dark twins and bright matrix, was gotten when matrix spots were used for dark field imaging. This observation was confirmed on several other foils. No evidence of a hcp epsilon phase was found by either electron or X-ray diffraction. Therefore it is concluded that the platelet structure is a result of deformation twinning which occurs after extensive cold work.

The dark field micrograph suggests (Fig. 8(*d*)) that the individual bands are not single isolated twins, but are packets of alternate thin layers of twinned and untwinned material. It also appears that the density of the packets increases with increasing deformation.

The cross-hatched structure shown in Figs. 4 and 5 is the result of several intersecting families of twin packets which are developed by extensive cold deformation.

DISCUSSION

The formation of fine twins during severe cold working can be attributed to both the relatively low stacking fault energy and the solid solution strengthening caused by a variety of substitutional elements in the alloy. The low stacking fault energy favors dislocation pile-ups and inhibits cross slip, while the solid solution strengthening results in hardening on the restricted deformation bands. There is ample evidence in the literature that these two effects contribute to twinning in fcc alloys.[4-9]

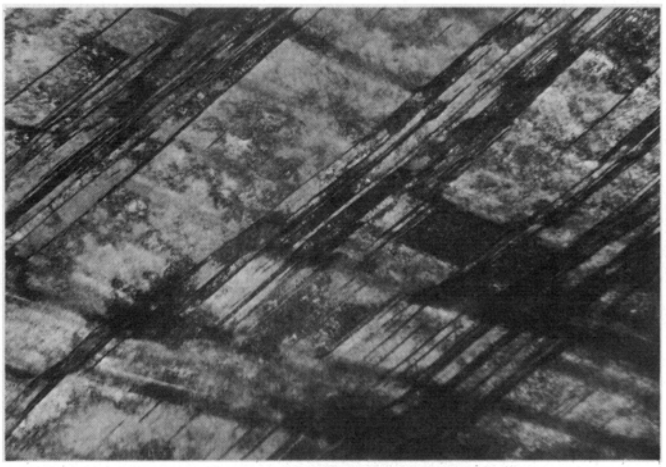

(a)

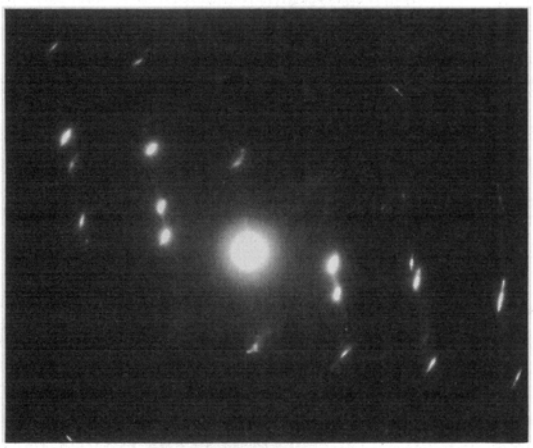

(b)

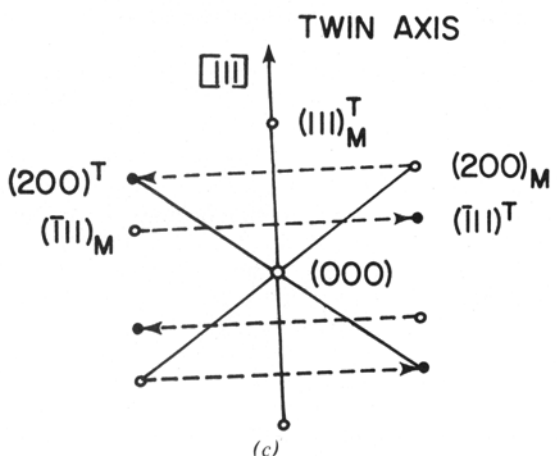

(c)

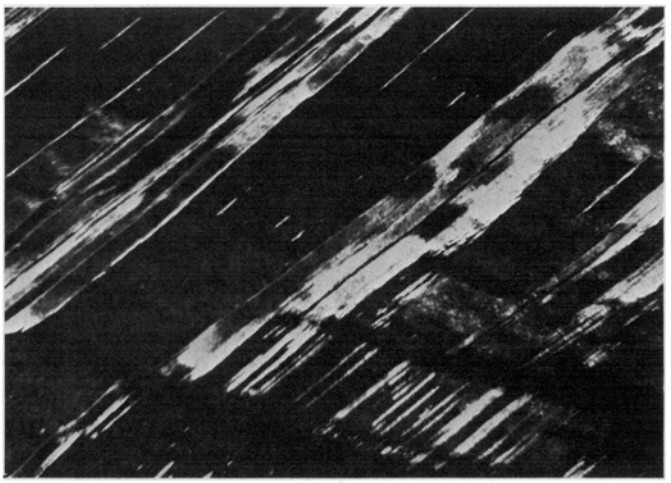

(d)

Fig. 8—(*a*) Bright field electron micrograph of an Fe-25 Ni-21 Co-20 Cr-8 Mo alloy after 48 pct deformation (by cold drawing) showing a lower than normal density of platelets. Magnification 15,000 times. (*b*) and (*c*) Electron diffraction pattern taken on the Fe-25 Ni-21 Co-20 Cr-8 Mo image in Fig. 8(*a*) (48 pct deformation by cold drawing). (*d*) Dark field electron micrograph of an Fe-25 Ni-21 Co-20 Cr-8 Mo alloy taken with twin reflection in Fig. 8(*b*) (48 pct deformation by cold drawing) showing the twins strongly diffracting. Magnification 15,000 times.

Mechanical twins have also been found in alloys in which strength is attributed to other factors besides substitutional solute element additions as Saito[10] and Michels *et al*[11] have reported in investigations of precipitation hardened copper-base alloys.

Venables,[4] Suzuki and Barrett,[5] and Haasen and King[6] demonstrated that alloying which reduces the stacking fault energy favors the nucleation of twins at lower stresses. In addition, Murr and Grace[12] have indicated that under shock loading, low stacking fault energy materials such as 18 Cr-8 Ni stainless steel (γ = 21 ergs/cm^2) and 70 Cu-30 Zn brass (γ = 21 ergs/cm^2) form planar type defects including linear dislocation arrays, stacking faults and twins, while high stacking fault energy metals such as aluminum (γ = 400 ergs/cm^2), nickel (γ = 300 ergs/cm^2) and copper (γ = 70 ergs/cm^2) develop dislocation cells and loops. This is also in agreement with the work of Hu and others[7,8] who attributed the increased incidence of twinning in fcc alloys to the lowering of stacking fault energy by alloying. These observations indicate that the low stacking fault energy of the experimental Fe-Ni-Co-Cr-Mo alloy would also favor twinning.

Murr and Grace[12] stated that, as a consequence of shock loading alpha brass, "It is apparent that the twin mode originates at higher degrees of cold work as an accommodation mechanism to relieve the shear developed in the elongated dislocation fields."

According to Venables,[4] a local stress concentration must exist at a twin source for twinning to occur. He also indicated that this stress concentration should be consistent with the work-hardening mechanism. As demonstrated in Fig. 2, linear dislocation arrays form most readily in this alloy and are thus available to act as stress concentrators.

Raghavan, Sastri, and Marcinkowski[13] observed, in a study of manganese Hadfield steel, that stacking faults, dislocations and twins, all of which are generated by plastic deformation, act as obstacles to one another. In addition the above authors[13] proposed that

in order to pass a dislocation through a mechanically twinned crystal, interfacial dislocations must be generated. Since this consumes energy, applied stress must be increased to maintain dislocation motion, thus accounting for high work-hardening rates.

Venables[4,9] also illustrated that twins form in profusion on a fine scale in highly alloyed low stacking-fault energy materials but propagate with difficulty through a forest of dislocations. This can account for the fine scale of twinning in the Fe-Ni-Co-Cr-Mo which, in addition to being a low stacking-fault material, is also highly alloyed. Deformation twins are said[12,13] to have the functional equivalence of a reduction in grain size in that they act as strong barriers to dislocation motions. As expected, they increase in effectiveness as twin density increases. It is reasonable to assume that the high density of fine twins shown in Fig. 5 could act as an obstacle to further dislocation movement and thus result in the high yield strength of 154 kg/mm^2 (219 ksi) observed in this alloy.

The deformed structure is remarkably similar to that found by others in iron-free Ni-Co-Cr-Mo alloys.[3,14] However, those authors[3,14] attributed the work strengthening to the formation of extremely thin platelets of hcp epsilon phase within the fcc matrix. The same investigators also found deformation twins in these alloys.

Mechanical twinning and the formation of an hcp phase have much in common. Raghavan *et al*[13] indicated that while the former is activated by strain energy and the latter by a chemical driving force, both are formed by stress, occur in an inhomogeneous manner and act as potential barriers to further plastic deformation.

The difference between a perfect fcc twin and a perfect hcp structure is one of stacking sequence. A succession of stacking faults on every (111) plane results in a fcc structure, while faulting on alternate (111) planes gives a hcp phase. Thus on an atomic scale, the difference between deformation twins and epsilon phase may be in degree of stacking rather than in type of structure. Murr and Grace[12] have presented a model which describes the formation of stacking faults, twin faults, hcp epsilon bundles and also bcc martensite in low stacking fault fcc materials on the basis of the propagation and interaction of partial dislocations. This illustrates that mechanistically, deformation-induced twins and hcp epsilon have a similar origin.

Drapier *et al*[3] point out that in MP35N the fcc-to-hcp phase change is rather sluggish and that the M_s temperature for this transformation may lie below room temperature. Graham and Youngblood[14] also characterized this fcc-to-hcp reaction as a diffusionless transformation and indicated that the temperature at which this occurs is decreased as the nickel content is increased. It is thus our opinion that hcp epsilon could possibly be formed in this high strength alloy by deforming below room temperature, although no evidence of its existence was found in this room temperature deformation study.

CONCLUSION

The high yield strength of 154 kg/mm^2 (219 ksi) attainable in this alloy as a result of 75 pct prior deformation is attributed to the large number of very fine mechanical twins which inhibit eacy dislocation motion.

ACKNOWLEDGMENT

The authors wish to express their appreciation to Dr. C. R. Cupp of INCO for his helpful criticisms of the manuscript.

REFERENCES

1. M. J. Whelan: *Proc. Roy. Soc.*, 1958, vol. A249, p. 114.
2. J. Friedel: *Dislocations*, p. 158, Pergamon Press, London, 1964.
3. J. M. Drapier, P. Viatour, D. Coutsouradis, and L. Habraken: *Cobalt*, 1970, no. 41, pp. 171-84.
4. J. A. Venables: *Deformation Twinning, Metallurgical Society Conferences*, vol. 25, pp. 77-110, Gordon and Breach, New York, 1964.
5. H. Suzuki and C. S. Barrett: *Acta Met.*, 1958, vol. 6, pp. 156-65.
6. P. Haasen and A. King: *A. Metallk.*, 1960, vol. 51, pp. 722-36.
7. H. Hu and R. S. Cline: *J. Appl. Phys.*, 1961, vol. 32, pp. 760-63.
8. H. Hu, R. S. Cline, and S. R. Goodman: *J. Appl. Phys.*, 1961, vol. 32, pp. 1392-99.
9. J. A. Venables: *Proc. European Regions Conf. on Electron Microscopy*, Vol. 1, pp. 443-46, Der Nederlandse Verenighing Voor Electronenmicroscopie, Delft, 1960.
10. K. Saito: *J. Phys. Soc. Jap.*, 1969, vol. 27, no. 5, pp. 1234-45.
11. H. T. Michels, I. B. Cadoff, and E. Levine: *Met. Trans.*, 1972, vol. 3, pp. 667-74.
12. L. E. Murr and F. I. Grace: *Trans. TMS-AIME*, 1969, vol. 245, pp. 2225-35.
13. K. S. Raghavan, A. S. Sastri, and M. J. Marcinkowski: *Trans. TMS-AIME*, 1969, vol. 245, pp. 1569-75.
14. A. H. Graham and J. L. Youngblood: *Met. Trans.*, 1970, vol. 1, pp. 423-30.